Journal of Vacuum Science and Technology A

RESEARCH ARTICLE | OCTOBER 01 2024

Low-loss and low-temperature Al_2O_3 thin films for integrated photonics and optical coatings

Special Collection: Multifunctional Coatings and Surfaces

Pooya Torab Ahmadi ; Michael Chesaux; Jacek Wojcik; Dino Deligiannis; Peter Mascher ; Jonathan D. B. Bradley

Check for updates

J. Vac. Sci. Technol. A 42, 063402 (2024)
https://doi.org/10.1116/6.0003976

View Online Export Citation

Articles You May Be Interested In

Transforming underground to surface mining operation – A geotechnical perspective from case study

AIP Conference Proceedings (November 2021)

Monthly prediction of rainfall in nickel mine area with artificial neural network

AIP Conference Proceedings (November 2021)

Estimation of Karts groundwater based on geophysical methods in the Monggol Village, Saptosari District, Gunungkidul Regency

AIP Conference Proceedings (November 2021)

01 October 2024 14:13:39

JVST A
Journal of Vacuum Science & Technology A

ARTICLE

pubs.aip.org/avs/jva

Low-loss and low-temperature Al_2O_3 thin films for integrated photonics and optical coatings

Cite as: J. Vac. Sci. Technol. A **42**, 063402 (2024); doi: 10.1116/6.0003976
Submitted: 12 August 2024 · Accepted: 12 September 2024 ·
Published Online: 1 October 2024

View Online Export Citation CrossMark

Pooya Torab Ahmadi,[1,a)] Michael Chesaux,[2] Jacek Wojcik,[2] Dino Deligiannis,[2] Peter Mascher,[1] and Jonathan D. B. Bradley[1]

AFFILIATIONS

[1]Department of Engineering Physics and Centre for Emerging Device Technologies, McMaster University, 1280 Main Street West, Hamilton, Ontario L8S 4L7, Canada
[2]Intlvac Thin Film, 247 Armstrong Avenue, Halton Hills, Ontario L7G 4X6, Canada

Note: This paper is a part of the 2024 Special Topic Collection on Multifunctional Coatings and Surfaces.
[a)]**Author to whom correspondence should be addressed:** torabahp@mcmaster.ca

ABSTRACT

Amorphous aluminum oxide (Al_2O_3) is a key material in optical coatings due to its notable properties, including a broad transparency window (ultraviolet to mid-infrared) and excellent durability. Moreover, its higher refractive index contrast relative to silica cladding layers and high solubility of rare-earth ions make it well suited for optical waveguides and the development of various functionalities in integrated photonics. In many coatings and integrated photonics applications, the substrates are temperature and stress sensitive, while relatively thick (~1 μm) alumina layers are required; thus, it is crucial to fabricate low optical loss alumina thin films at low deposition temperatures, while maintaining high deposition rates. In this study, plasma-assisted reactive magnetron sputtering, operated in an alternating current mode, is investigated as a reliable, straightforward, and wafer-scale compatible technique for the deposition of high optical quality and uniform Al_2O_3 thin films at low temperature. One-micrometer-thick amorphous Al_2O_3 planar waveguides, deposited at 150 °C and a rate of 23.3 nm/min, exhibit optical losses below 1 dB/cm at 638 nm and as low as 0.1 dB/cm in the conventional optical communication band.

Published under an exclusive license by the AVS. https://doi.org/10.1116/6.0003976

01 October 2024 14:13:39

I. INTRODUCTION

Optical thin film coatings play a pivotal role in a wide array of modern photonics applications. Such coatings are composed of nanoscale layers of materials with specific optical properties, offering precise control over light interactions within a certain wavelength range. Recent advancements in thin film technology allow for the fabrication of sophisticated coating designs with considerable flexibility in adjusting the properties of the optical layers, facilitating applications ranging from spectroscopic filters and photovoltaics to sensors and biomedical devices.[1,2] Integrated photonics is among the technologies that benefit from advancements in optical thin film coating techniques. Integrated photonics aims to create reliable compact optical circuits, mirroring the impact of electronic integrated circuits on the photonics industry. Achieving this objective necessitates the precise fabrication of individual photonic components with desired properties, typically requiring the use of expensive and sophisticated methods and processes.[3] Using existing complementary metal-oxide semiconductor (CMOS) fabrication facilities has been an effective approach for reducing the costs and complexities of fabricating these components.[4–6] However, fabrication methods intended for use in this category are subject to particular constraints, including temperature sensitivity, material compatibility, cost factors, and fabrication speed. Additionally, industrial-scale production requires wafer-scale fabrication with high reproducibility, uniformity, and full automation.[2,7]

Among the multitude of materials used for the advancement of integrated photonics, amorphous aluminum oxide (Al_2O_3) has attracted significant attention. Amorphous Al_2O_3 has excellent thermal, chemical, and mechanical stability. Its moderately high refractive index (~1.65 at 633 nm) with a contrast of approximately 0.2 compared to silicon dioxide (SiO_2), high rare-earth ion solubility, and a wide transparency window from ultraviolet to mid-infrared make it an ideal platform for the development of passive and active optical components in integrated photonics, including waveguides,[8–13] lasers,[14–16] and amplifiers.[17,18]

Published under an exclusive license by the AVS

Various chemical and physical deposition methods have been used for the fabrication of amorphous Al_2O_3 optical thin film coatings, including sol-gel, chemical vapor deposition (CVD), pulsed laser deposition (PLD), atomic layer deposition (ALD), and reactive sputtering. The films fabricated through sol-gel and CVD processes often exhibit relatively higher optical propagation losses and luminescence quenching due to the high amount of OH^- introduced during the fabrication process.[11,14,17,19] Although liquid removal and film densification can be achieved through subsequent heat treatment, this often necessitates using high temperatures, which may not be acceptable for delicate or temperature-sensitive substrates.[1,12,18,20,21] Thus, the films fabricated with these methods are not usually suitable for use in many passive and active optical applications. In ALD, the thin film deposition process occurs through sequential exposure of a substrate to alternating gaseous precursors. Each precursor reacts with the surface in a self-limiting manner, enabling deposition of a single atomic layer at a time. Despite the presence of OH groups in ALD films, the superior film uniformity and density achieved through this technique result in high optical quality films with low propagation losses. However, its slow deposition rate, costly process, and high complexity make it less suitable for large-scale production, particularly for thick layers.[1,12–14,18,22,23] High-quality thin films with controlled stoichiometry can also be achieved by using PLD. PLD employs laser pulses to ablate a target material within a vacuum chamber, and it is mostly considered a laboratory-scale technique. A small coating area with acceptable uniformity and low deposition rates are the most important challenges of this fabrication method.[2,17,19]

Reactive sputtering has been established as a highly suitable method to deposit low-loss Al_2O_3 films. In reactive sputtering of Al_2O_3, an aluminum metal target is bombarded by high-energy ions, and the collision between these ions and the target atoms results in material ejection. Subsequently, a chemical reaction between the ejected aluminum atoms and the reactive O_2 gas inside the chamber leads to the formation of a compound Al_2O_3 film on the substrate.[3,14] Although reactive sputtering also offers a reasonable level of control over the film properties, it is often considered less complex than PLD and ALD techniques. Reactive sputtering also typically provides higher deposition rates in contrast to PLD and ALD. Its relative simplicity aligns well with industrial production requirements and allows for appropriate integration with wafer-scale fabrication processes.[14] Among various reactive sputtering techniques, radio frequency (RF) magnetron sputtering has become the most prominent method for fabrication of Al_2O_3 thin films with low optical propagation loss for integrated photonics. Its ability to sustain a plasma state, without inducing a heavy charge buildup, helps in achieving uniform and high-quality optical thin films. Nonetheless, many studies on RF sputtering deposition of alumina thin films have indicated the need for deposition temperatures above 400 °C or postdeposition annealing between 500 and 800 °C to minimize the propagation loss of the film.[8,9,14,17,19,22,24–27] This requirement can increase the complexity of fabrication and constrain its applicability, particularly when seeking compatibility with temperature-sensitive substrates. In an effort to fabricate CMOS-compatible Al_2O_3 thin films, Magden *et al.* demonstrated a substrate-bias-assisted sputtering method for low-loss alumina deposition at a lower temperature of 250 °C by applying a high substrate bias of 90 W.[28] However, this method presents challenges, as even small temperature changes (±20 °C) can drastically increase film propagation loss due to cluster-void and nanocrystal formations at lower and higher deposition temperatures, respectively, potentially leading to reliability issues. Additionally, it should be noted that the highest deposition rate reported for low-loss alumina deposition in previous studies is below 6 nm/min, which may further limit its practical application in large-scale production.[9,17,19,25,28]

Recently, plasma-assisted reactive magnetron sputtering (PARMS) has emerged as a promising deposition technique for optical thin film fabrication.[29–32] Unlike conventional magnetron sputtering, which primarily relies on the Ar plasma around the magnetron sputtering gun for ion formation, PARMS uses an additional plasma source to activate both the reactive gas, such as O_2, and part of the Ar gas introduced into the deposition chamber. This supplementary plasma source enhances the reactivity and energy of the ions, promoting more efficient film formation. Furthermore, introducing a significant current of low-energy ions (<100 eV) via this plasma source into the deposition process, along with maintaining a low process pressure, effectively counteracts the formation of voids and removes the adsorbed water molecules on the substrate.[2] This results in the fabrication of dense microstructures and smooth layers with minimal roughness, leading to low optical losses. Consequently, PARMS can achieve higher film quality at lower deposition temperatures compared to traditional reactive magnetron sputtering methods. Additionally, the ion source can also be used as a simple and cost-effective method for substrate precleaning, which is often one of the important requirements for advanced optical thin film coatings. This process enhances the film adhesion to the substrate and minimizes defects in the deposited films.[2,30,32,33] Despite the proven capabilities of PARMS for depositing low-loss planar waveguides,[29] there are few studies exploring its use for alumina deposition in waveguide applications. These studies report relatively high propagation losses, above 25 dB/cm at 633 nm and 4–10 dB/cm at 1550 nm, making them unsuitable for state-of-the-art waveguide applications.[31]

In this work, an alternating current (AC) PARMS system is employed as an advanced fabrication technique for depositing low-loss Al_2O_3 thin films at low temperatures. Structural and morphological analyses were conducted to assess the crystallinity, stoichiometry, and surface roughness of the deposited Al_2O_3 thin films. Additionally, various optical measurements were performed to determine the refractive index and propagation loss of the films across various wavelengths within the visible and near-infrared regions. The results demonstrate the feasibility of fabricating low-loss amorphous alumina thin films with stoichiometric composition, very low surface roughness, high thickness uniformity, and high deposition rates at 150 °C using this deposition method. This is promising for the fabrication of high optical quality thin film coatings on large temperature-sensitive substrates and the development of advanced optical devices in integrated photonics.

II. EXPERIMENT

A. Al_2O_3 deposition with a PARMS system

An Intlvac Nanochrome IV PARMS system was used in this study. A schematic of the deposition chamber with its key

01 October 2024 14:13:39

Published under an exclusive license by the AVS

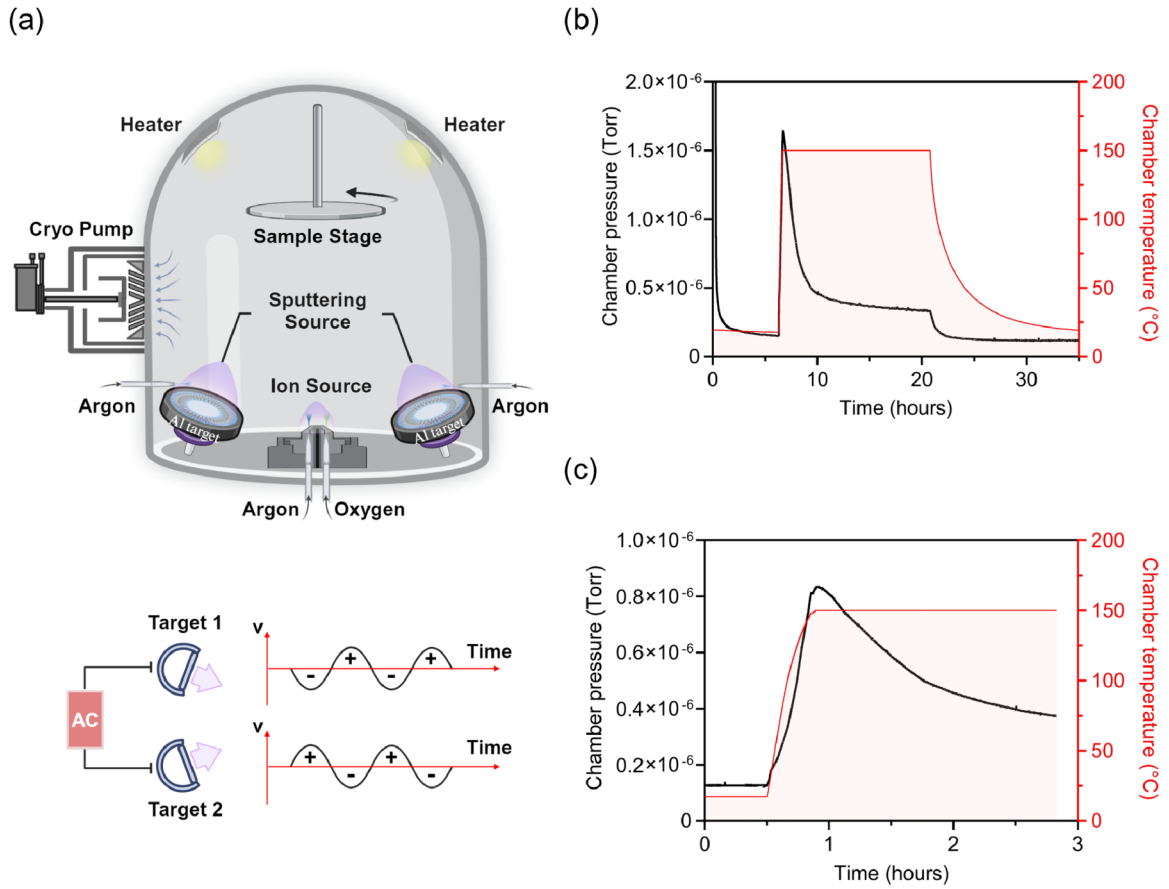

FIG. 1. (a) Schematic of the PARMS system using dual AC power supply (the positions of components are not-to-scale and are not indicative of their actual arrangement). (b) 14 h heating at 150 °C after each pump-down cycle to enhance film purity by reducing the base pressure through the removal of released gases. (c) Outgassing by 2 h heating at 150 °C before each deposition run to achieve optimal condition for the film deposition.

components is illustrated in Fig. 1(a). It comprises an ion source and two 6-in. diameter aluminum metal sputtering targets with 99.999% purity. The system uses a cryogenic pump for chamber evacuation, effectively reducing the base pressure to 1.2×10^{-7} Torr. Sputtering was performed using a dual AC power supply set at a power of 1300 W. The deposition process was carried out at a process pressure of 8×10^{-4} Torr with high-purity argon at a flow rate of 80 sccm to create the plasma. A reactive environment for the formation of Al_2O_3 thin films on the substrate was established using a 99.993% pure O_2 flow. In order to determine the optimum O_2 flow rate for stoichiometric Al_2O_3 films, the target's bias response to the O_2 flow rate was monitored. The substrate temperature during deposition was maintained at 150 °C, and the substrate rotation speed was set at 30 rpm to promote uniform film growth.

Pieces of a silicon wafer and a thermally oxidized silicon wafer, of suitable dimensions, were used as substrates. The substrates were cleaned by immersion in acetone for 2 min, subsequent rinsing with isopropanol, and drying using a nitrogen gas gun prior to loading them into the system. Before starting the deposition process, precleaning and outgassing steps were carried out to reduce contamination inside the chamber and on the substrate, particularly water molecules. In order to ensure the purity of the deposited films, the chamber was heated for 14 h at 150 °C after the first pump-down cycle to reduce the base pressure at room temperature from 1.5 $\times 10^{-7}$ to 1.2×10^{-7} Torr by eliminating released gases [Fig. 1(b)]. This extended heating step is used to accelerate the initial outgassing following any chamber exposure to atmosphere for maintenance activities, such as target changes or cleaning, and is not required for subsequent deposition runs. In routine operations, where the chamber remains sealed and substrates are transferred via a load-lock, the chamber was heated for 2 h at 150 °C before each deposition run until a pressure lower than 4×10^{-7} Torr at 150 °C was reached [Fig. 1(c)]. This careful outgassing procedure creates an optimal environment for the deposition of high-quality and low-loss coatings by removing moisture and contaminants introduced during the load-lock transfer. This step is particularly important in humid environments, and it can be

01 October 2024 14:13:39

Published under an exclusive license by the AVS

optimized and shortened in cleanrooms with humidity and contamination controls. Finally, a 10 min substrate precleaning step was performed with argon ions using the ion source. This precleaning step is optional and can be omitted from the deposition process when working with sensitive substrates.

To determine a suitable Al_2O_3 deposition recipe with the PARMS system, it is important to understand the fundamentals of dual AC reactive magnetron sputtering. In magnetron sputtering, a plasma is generated over the target surface by applying a negative bias to the target. The presence of a magnetic field confines the plasma close to the target's surface, enhancing the sputtering efficiency and the deposition rate. In this condition, positively charged ions of an inert gas, typically argon, from the plasma bombard the negatively biased target surface and cause the ejection of target material atoms. The ejected atoms subsequently condense on the substrate and form a thin film. In direct current (DC) sputtering, applying continuous DC power to the magnetron targets can lead to charge buildup, which increases the likelihood of arcing during the sputtering process. Unlike DC magnetron sputtering, where a continuous DC power supply is used, AC magnetron sputtering involves alternating current. In dual AC magnetron sputtering, two magnetron targets are connected to an AC power supply, and the cathode and anode alternate between the two targets every half cycle. This alternating mechanism prevents charge buildup on the targets during the sputtering process, which results in a highly stable sputtering process free from arcing.[1,34,35]

Reactive sputtering of Al_2O_3 thin films requires maintaining an appropriate flow of oxygen gas into the chamber, aside from the presence of the inert gas (argon), to create a proper condition for the Al_2O_3 reaction.[14] The reactive gas, oxygen in this case, is not only consumed by the pump but also reacts with the growing film on the substrate and the newly exposed material on the chamber shields and the sputtering targets, where the material was deposited or etched. On the target, there is a competition between the rate of an oxygen reaction with the surface and the rate at which oxygen is sputtered off from the surface by argon ions. Once the oxygen pressure exceeds a critical point inside the chamber, the gettering capacity in the reaction chamber becomes saturated, and most of the target surfaces will be covered with an insulating oxide layer, known as target poisoning. The presence of this oxide layer on the target surface typically reduces the sputter rate and limits the exposure of fresh surfaces for a further reaction with oxygen. This creates a reinforcing feedback loop, causing the process to transition from a metallic mode to a poisoned mode. The tipping point between these two modes can vary depending on whether the process begins in the poisoned mode, where oxidation dominates the reaction, or in the metallic mode, where the speed of fresh material exposure prevails. This phenomenon is referred to as hysteresis, characterized by the dependency of the system's state on its history. The change in the sputter target surface condition can impact certain operational parameters by affecting the plasma's electrical properties, particularly the target bias voltage delivered by the power supply at a fixed sputtering power. The width of this hysteresis region is associated with the competition between the oxygen consumed by the pump or reacted with freshly exposed surfaces. Understanding and controlling this phenomenon are crucial for ensuring the desired optical layer properties. Accordingly, the O_2 flow rate and other process parameters were adjusted and monitored during deposition to prevent a reduction in the deposition rate and maintain overall film quality.[14,34,36]

B. Thin film characterization

1. Structure and compositional analyses

To examine the composition of the deposited films, Rutherford backscattering spectrometry (RBS) with a 2.0 MeV $^4He^+$ ion beam in a Cornell geometry and a dose of 2 μC was employed. The RBS data were modeled using the SIMNRA software package to determine the composition ratio of the alumina thin films. X-ray diffraction (XRD) data of the Al_2O_3 thin films were collected using a Bruker D8 Discover XRD system with a DAVINCI design diffractometer equipped with a cobalt source (λ_{avg} = 1.79026 Å) and an Eiger2 R 500 K area detector. A coupled 2D continuous scan, with 0.02° steps and a scan speed of 0.3 s per step, was used to collect a 2θ scan range from 10° to 90°. The collected data were analyzed using DIFFRAC.EVA software.

2. Optical characterization

For the determination of Al_2O_3 film thickness and refractive indices, a J. A. Woollam M-2000 variable angle spectroscopic ellipsometer (VASE) was used. Spectra were collected at angles of 55°, 60°, 65°, 70°, and 75° from the surface normal and analyzed using COMPLETEEASE software. The obtained data were modeled and fit to extract optical constants in the range of 400–1680 nm. The optical propagation losses of the deposited amorphous alumina thin films on thermal oxide silicon wafers were measured using a Metricon 2010/M prism coupler at wavelengths of 638, 847, 1310, 1450, 1550, and 1650 nm. Multiple loss measurements were performed on different regions of the wafer, and the average value was taken.

3. Surface topography analysis and a thickness uniformity measurement

The surface roughness of an Al_2O_3 thin film deposited on a thermally oxidized silicon wafer was evaluated using Bruker Dimension Icon atomic force microscopy (AFM) in a tapping mode in air. The measurements were conducted by using an FESPA-V2 tip with a nominal frequency of 75 kHz and a stiffness of 2.8 N/m. Root-mean-squared roughness (Rq) values were determined by sampling three random 2.5 × 2.5 μm^2 areas on the surface and analyzed using BRUKER NANOSCOPE software. To investigate the deposition uniformity, thickness and refractive index mappings were performed on a 3-in. silicon wafer using a Philips PZ2000 ellipsometer equipped with a 633 nm laser.

4. Mechanical testing

To evaluate the adhesion and abrasion resistance of the deposited alumina coatings, the films were tested according to specific industrial coating standards. In the adhesive test, a 50 mm strip of a standard pressure sensitive adhesive tape was firmly applied across the surface of the test area. Then, the tape was swiftly removed with a rapid upward pull force, oriented approximately

01 October 2024 14:13:39

Published under an exclusive license by the AVS

perpendicular to the test area. The coating passes the test successfully if no evidence of coating removal is observed after the tape removal. For severe abrasion resistance assessment, a designed pen shape brass tool equipped with a 2½ lb spring was used. A specific eraser attached to the top of the tester was used to repeatedly rub the coated surface with 1-in. strokes for a total of 20 complete strokes, all confined to a single path. Following the abrasion test, the surface of the coating was cleaned with acetone and carefully inspected for any signs of material removal or scratches, which would indicate test failure. As a final step, a KLA Tencor P-16$^+$ stylus profiler was used for thin film stress measurements. Predeposition and postdeposition scans were collected along a 6-cm length of the 3-in. silicon wafer, with a scan rate of 400 μm/s, a sampling rate of 15 Hz, and an applied force of 2.0 mg. The change in the substrate's radius of curvature resulting from the film deposition was calculated with a fifth order polynomial fit.

5. Annealing study

To investigate the impact of annealing on the optical propagation loss of the amorphous alumina thin films, a sample was annealed at 400 and 600 °C for 4 h under a continuous N_2 gas flow, consistent with the reported crystallization temperature of alumina films, which is above 800 °C.[13,33] Optical propagation loss measurements, structural analysis, and surface roughness imaging were conducted on the annealed samples to examine potential effects of annealing on the Al_2O_3 film properties.

III. RESULTS AND DISCUSSION

As an initial step in optimizing the deposition process, the target bias voltage hysteresis curve was investigated to explore the dynamic interaction between the voltage of the aluminum targets and the O_2 flow rate, providing insights into plasma behavior throughout the deposition process. Precisely selecting the O_2 flow rate enables the control of stoichiometry, deposition rate, and the optical properties of the Al_2O_3 thin film, including the refractive index, optical transmission/reflection characteristics, and optical propagation loss within the film. The meticulous adjustment of the O_2 flow is crucial for tailoring the film properties to meet specific requirements in different optical applications.[19,26,37]

Figure 2(a) illustrates the hysteresis behavior of the aluminum target voltage observed across varying oxygen flow rates in the reactive sputtering process. The deposition rate calculation in the inset

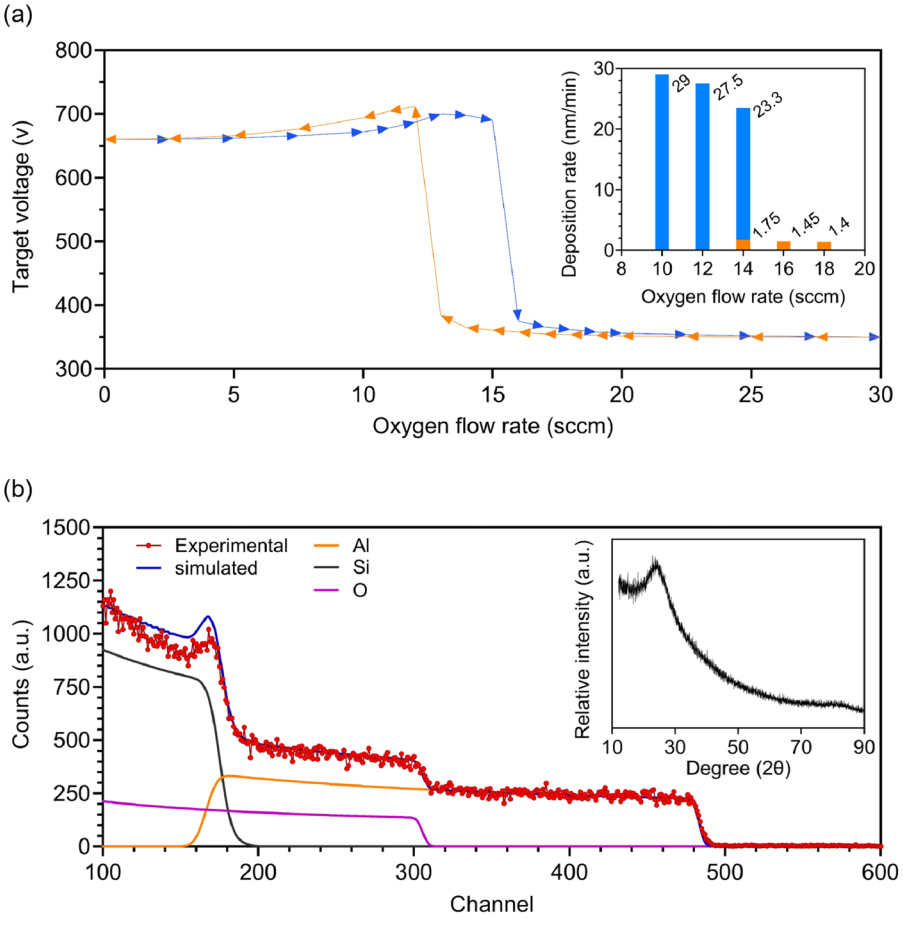

FIG. 2. (a) The hysteresis behavior of an aluminum target voltage vs an oxygen flow rate in the reactive sputtering process. The inset shows the deposition rate as a function of oxygen flow rate. (b) RBS experimental spectrum with corresponding simulation model fits for oxygen, aluminum, and silicon. Inset in B: XRD spectrum of an Al_2O_3 thin film deposited at 150 °C with the O_2 flow of 14 sccm showing the amorphous structure of the film.

01 October 2024 14:13:39

Published under an exclusive license by the AVS

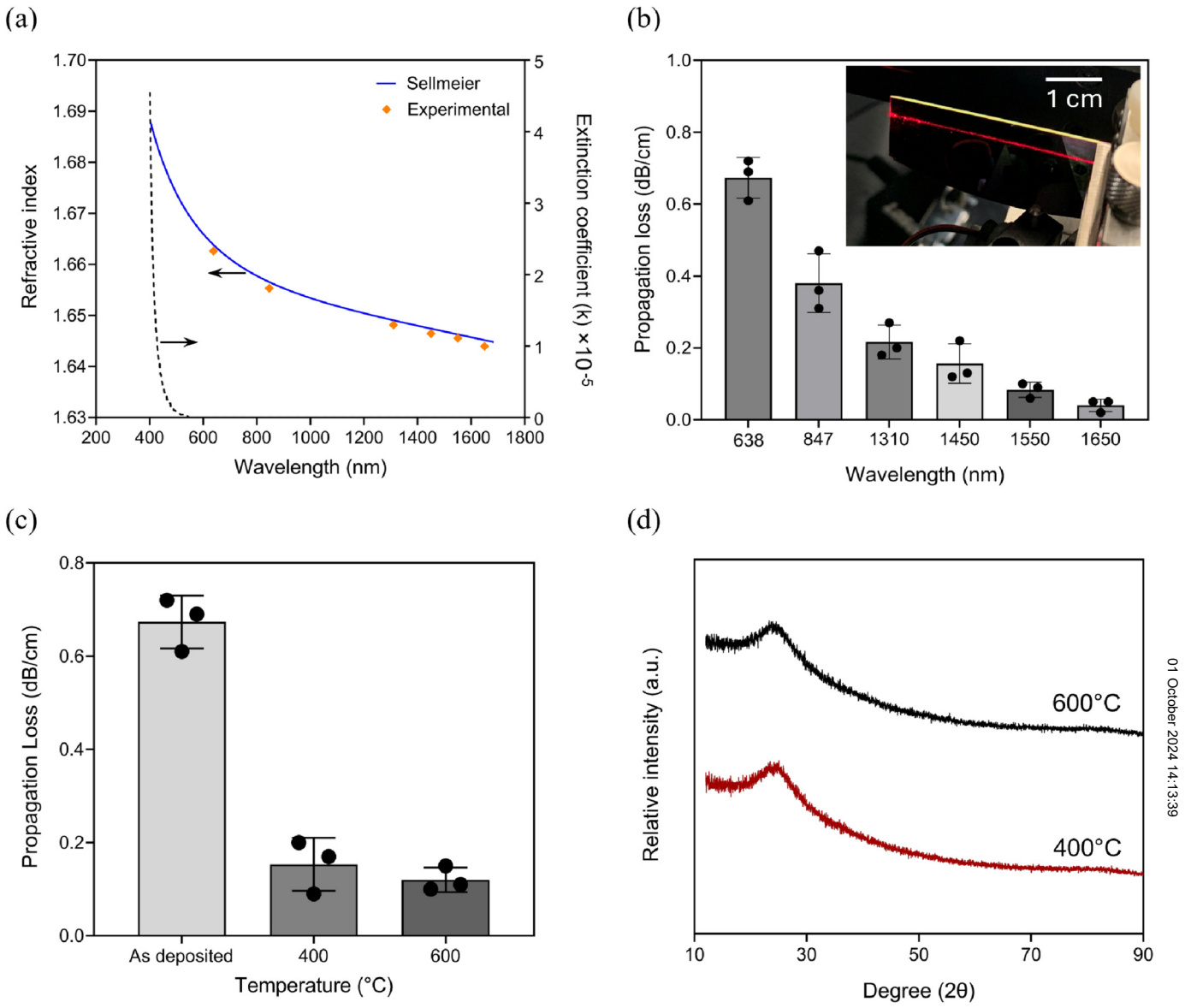

FIG. 3. (a) Refractive index and the extinction coefficient of an Al_2O_3 thin film as a function of wavelength in the range of 400–1680 nm, measured with VASE and a prism coupler. (b) Propagation losses of the Al_2O_3 thin film in the range of 638–1650 nm measured by a prism coupling method. (c) Impact of postdeposition annealing at 400 and 600 °C for 4 h on the propagation loss at 638 nm. (d) XRD spectra of the annealed alumina thin film at 400 and 600 °C for 4 h.

of this figure demonstrates a significant change within the hysteresis area, in transition from the metal side with a higher bias voltage to the oxide region with a lower bias voltage. Target surface oxidation at high oxygen pressures leads to different deposition rates at the same O_2 flow rate within the hysteresis region, depending on the previous condition of the targets. For instance, at an oxygen flow rate of 14 sccm, two different deposition rates of 23.3 nm/min and 1.75 nm/min are observed. Thus, the target voltage serves as an indicator of the extent of oxidation on the targets.

Given the importance of achieving a high deposition rate, our focus was on directing the film deposition process toward the metal side of the hysteresis curve, characterized by a higher target voltage. However, a minimum oxygen pressure is essential for achieving a stoichiometric reactive environment. Therefore, due to the lower oxygen pressure in this particular region, the deposition process must be performed very close to the transition point, often referred to as the sputtering knee point.[14] This approach is essential not only to achieve a high deposition rate but also to attain a

01 October 2024 14:13:39

Published under an exclusive license by the AVS

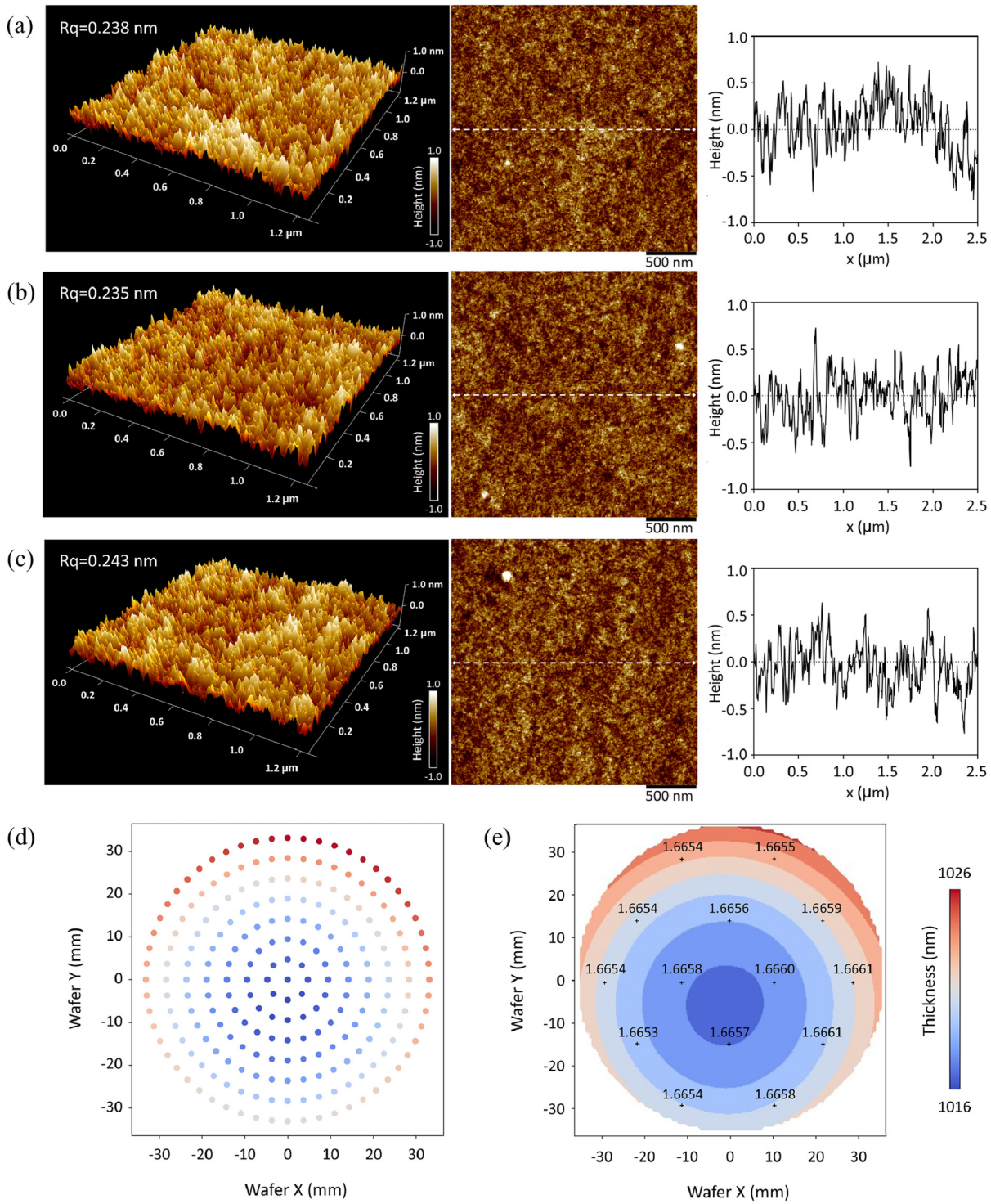

FIG. 4. 2D and 3D images of the surface morphology and the height profile across 2.5 μm acquired by AFM for the (a) as-deposited Al_2O_3 film, (b) the Al_2O_3 film annealed at 400 °C for 4 h, and (c) the Al_2O_3 film annealed at 600 °C for 4 h. (d) Uniformity assessment of Al_2O_3 film thickness and (e) a refractive index (overlaid on top of the measured film thickness mapping) measured across a 3-in. silicon wafer.

01 October 2024 14:13:39

Published under an exclusive license by the AVS

stoichiometric Al_2O_3 thin film.[19] In this region, the target surface maintains its metallic nature, while there is a sufficient oxygen content to facilitate oxidic deposition. It is worth noting that deposition near the knee point can be challenging, as the deposition process can drift during the deposition. Nevertheless, in this study, relatively stable voltage behavior was observed at the oxygen flow rate of 14 sccm. Therefore, an automated proportional-integral-derivative (PID) control mechanism was not employed for adjusting the voltage by varying the oxygen flow. It is important to emphasize that for extended deposition processes, the implementation of PID control can enhance the stability of the deposition parameters throughout the process. This stability is crucial for achieving reproducible sputtered layers throughout the lifetime of the sputtering target, particularly in large-scale fabrication.

RBS characterization of an Al_2O_3 thin film deposited at an oxygen flow rate of 14 sccm revealed that the deposited film has a close-to-stoichiometric composition, as depicted in Fig. 2(b). The analysis of the RBS spectra demonstrates a strong agreement between the experimental data and the simulated stoichiometric alumina composition, indicating a nearly ideal ratio of aluminum and oxygen atoms in the deposited film. Furthermore, XRD measurement, shown in the inset of Fig. 2(b), verified the amorphous nature of the deposited films. According to the XRD results, the Al_2O_3 thin film retains its noncrystalline state throughout the deposition process at 150 °C.

To evaluate the optical properties of the deposited alumina films, spectroscopic ellipsometry and prism coupling tests were conducted to determine their refractive indices and propagation losses over the visible and near-infrared wavelengths. Figure 3(a) shows the refractive index and the extinction coefficient of an Al_2O_3 film as a function of wavelength in the range of 400–1680 nm. The Sellmeier and the General Oscillator models were applied to the data obtained from VASE to analyze the optical constants of the alumina thin film. Comparing the dispersion curves generated by Sellmeier model with the refractive indices directly measured via prism coupling showed close agreement between the measured indices and the model outputs.

As shown in Fig. 3(b), we obtain low-loss alumina thin films using the PARMS technique at a low temperature. These losses are comparable to those reported for alumina thin films deposited using other methods.[9,11,12,14,17,18,25] The film exhibits optical losses of approximately 0.67 dB/cm at 638 nm and as low as 0.1 dB/cm at 1550 nm, which makes it a promising candidate for applications in the communication C-band wavelength region. Importantly, these low propagation losses were obtained without any subsequent heat treatment, highlighting the practicality and efficiency of the PARMS approach in fabrication of high-quality optical coatings for temperature-sensitive substrates. However, for nontemperature-sensitive substrates, propagation losses can be further reduced through postdeposition annealing at elevated temperatures below the crystallization point.[9,14,33] Figure 3(c) illustrates that annealing at 400 and 600 °C for 4 h reduces the propagation loss at 638 nm to less than 0.2 dB/cm. XRD analysis [Fig. 3(d)] confirmed that the films remain amorphous after annealing, with no discernible crystalline peaks.

Figure 4 depicts the surface topography of the 1 μm-thick alumina thin film before and after annealing. The AFM images and the height profile demonstrate a uniform and smooth surface, with an average roughness (Rq) of 0.238 nm in the as-deposited sample [Fig. 4(a)]. In our previous study,[29] we observed that annealing contributed to a reduction in the surface roughness of the deposited film, along with a weak correlation between the surface roughness and the propagation loss. Several studies have suggested that annealing reduces propagation loss by densifying the film, inducing stoichiometric changes, or relieving residual film stresses caused by deposition.[9,21,22,38] However, these trends were not evident in the current study. The films annealed at 400 and 600 °C exhibited no significant roughness changes in comparison with the as-deposited films [Figs. 4(b) and 4(c)]. In addition, our observations did not show any significant alterations in film thickness or stoichiometry after annealing. Furthermore, thin film stress measurements on the as-deposited thin films ranged from 6 MPa (tensile) to −19 MPa (compressive), indicating very low stress levels within the deposited films. Therefore, a more in-depth investigation is needed to explain the specific mechanisms responsible for the impact of annealing on propagation loss.

Given that one of the objectives in this study was the evaluation of the capability of using this method for industrial-scale coating applications, the mechanical and uniformity characteristics of the deposited films were of great importance. The deposited alumina thin films were inspected to assess their adhesion and abrasion resistance. These tests showed no evidence of coating removal in the adhesive test, and minimal material removal or scratches after a severe abrasion resistance assessment. Moreover, the thickness and refractive index mapping graphs presented in Figs. 4(d) and 4(e) show less than 0.8% and 0.05% total thickness and refractive index variation across a 3-in. wafer located approximately at the center of the substrate, respectively, highlighting the high uniformity achieved during the deposition process. While a 3-in. wafer was used in this study, this deposition system is capable of handling a 10-in. wafer, up to seven 3-in. wafers, or three 4-in. wafers per run, with a thickness uniformity variation of less than 2% for various oxide and nitrides.[39] This makes the system well suited for batch and large-diameter wafer productions at an industrial scale.

IV. SUMMARY AND CONCLUSIONS

Amorphous stoichiometric Al_2O_3 thin films with high optical quality have been fabricated by dual AC plasma-assisted magnetron sputtering at 150 °C and a deposition rate of 23.3 nm/min. The planar waveguide of the as-deposited film exhibits propagation losses of 0.67 dB/cm at 638 nm and as low as 0.1 dB/cm across the conventional optical communication band, making it highly suitable for near-infrared applications, particularly in integrated photonics. Moreover, annealing of the deposited films demonstrates the potential for a further reduction in propagation losses. The deposited thin films exhibit acceptable adhesion and abrasion resistance, with minimal surface roughness (Rq~0.24 nm) and less than 1% thickness variation over a 3-in. wafer. This reliable and highly stable deposition technique shows great potential for large-scale production of advanced optical coatings, making it suitable for a wide range of applications.

01 October 2024 14:13:39

Published under an exclusive license by the AVS

ACKNOWLEDGMENTS

This work was supported by the Mitacs Accelerate program (No. IT23542) and the Ontario Research Foundation (No. ORF-RE 09-051). The authors express their gratitude to Deanna Reyes and Peter J. Van Nooten from the Intlvac Thin Film for their assistance with mechanical tests, as well as Victoria M. Jarvis for her assistance with x-ray analyses. The authors would also like to acknowledge the Center of Emerging Device Technology (CEDT), the Analytical X-Ray Diffraction Facility (MAX), and the Centre for Advanced Light Microscopy (CALM) at McMaster University, and Western University's Tandetron Laboratory for providing access to their equipment and recourses.

AUTHOR DECLARATIONS

Conflict of Interest

The authors have no conflicts to disclose.

Author Contributions

Pooya Torab Ahmadi: Conceptualization (lead); Data curation (lead); Formal analysis (lead); Investigation (lead); Methodology (lead); Validation (equal); Visualization (lead); Writing – original draft (lead); Writing – review & editing (lead). **Michael Chesaux:** Conceptualization (supporting); Methodology (supporting); Supervision (supporting); Validation (equal); Writing – review & editing (supporting). **Jacek Wojcik:** Project administration (equal); Writing – review & editing (supporting). **Dino Deligiannis:** Funding acquisition (equal); Resources (equal). **Peter Mascher:** Conceptualization (supporting); Funding acquisition (equal); Methodology (supporting); Resources (equal); Supervision (lead); Validation (equal); Writing – review & editing (equal). **Jonathan D. B. Bradley:** Conceptualization (equal); Funding acquisition (equal); Methodology (supporting); Project administration (equal); Resources (equal); Supervision (lead); Validation (equal); Writing – review & editing (equal).

DATA AVAILABILITY

The data that support the findings of this study are available from the corresponding author upon reasonable request.

REFERENCES

[1]A. Piegari and F. Flory, *Optical Thin Film and Coatings—From Materials to Applications* (Woodhead, Sawston, Cambridge, 2013).
[2]D. Ristau and H. Ehlers, *Springer Handbook of Lasers and Optics—Thin Film Optical Coatings* (Springer, New York, 2007).
[3]M. A. Butt *et al.*, Materials **15**, 4591 (2022).
[4]J. M. Fedeli, L. Di Cioccio, D. Marris-Morini, L. Vivien, R. Orobtchouk, P. Rojo-Romeo, C. Seassal, and F. Mandorlo, Adv. Opt. Technol. **2008**, 412518 (2008).
[5]A. H. Atabaki *et al.*, Nature **556**, 349 (2018).
[6]G. T. Reed, Nature **427**, 595 (2004).
[7]P. M. Solomon, Annu. Rev. Mater. Sci. **30**, 681 (2000).
[8]J. J. Díaz Leon, D. M. Fryauf, J. E. Volk, and N. P. Kobayashi, IEEE Photonics Technol. Lett. **31**, 43 (2019).
[9]M. K. Smit, G. A. Acket, and C. J. van der Laan, Thin Solid Films **138**, 171 (1986).
[10]S. Garcia-Blanco, W. Hendricks, D. Bonneville, S. Mardani, and M. Dijkstra, "UV integrated photonics in sputter deposited aluminum oxide," Opt. Open (to be published).
[11]K. Worhoff, F. Ay, and M. Pollnau, ECS Trans. **3**, 17 (2006).
[12]M. M. Aslan, N. A. Webster, C. L. Byard, M. B. Pereira, C. M. Hayes, R. S. Wiederkehr, and S. B. Mendes, Thin Solid Films **518**, 4935 (2010).
[13]G. N. West, W. Loh, D. Kharas, C. Sorace-Agaskar, K. K. Mehta, J. Sage, J. Chiaverini, and R. J. Ram, APL Photonics **4**, 026101 (2019).
[14]W. A. P. M. Hendriks, L. Chang, C. I. van Emmerik, J. Mu, M. de Goede, M. Dijkstra, and S. M. Garcia-Blanco, Adv. Phys. X **6**, 1 (2021).
[15]M. de Goede, L. Chang, J. Mu, M. Dijkstra, R. Obregón, E. Martínez, L. Padilla, F. Mitjans, and S. M. Garcia-Blanco, Opt. Lett. **44**, 5937 (2019).
[16]J. D. Bradley, R. Stoffer, L. Agazzi, F. Ay, K. Wörhoff, and M. Pollnau, Opt. Lett. **35**, 73 (2010).
[17]K. Wörhoff, J. D. B. Bradley, F. Ay, D. Geskus, T. P. Blauwendraat, and M. Pollnau, IEEE J. Quantum Electron. **45**, 454 (2009).
[18]M. Demirtas, C. Odaci, N. K. Perkgoz, C. Sevik, and F. Ay, IEEE J. Sel. Top. Quantum Electron. **24**, 1 (2018).
[19]C. I. van Emmerik *et al.*, Opt. Mater. Express **10**, 1451 (2020).
[20]T. Ishizaka, Y. Kurokawa, T. Makino, and Y. Segawa, Opt. Mater. **15**, 293 (2001).
[21]M. Mahnke, S. Wiechmann, H. J. Heider, O. Blume, and J. Müller, AEU-Int. J. Electron. Commun. **55**, 342 (2001).
[22]S. Chen, L. Tao, L. Zeng, and R. Hong, Int. J. Photoenergy **2013**(1), 792357 (2013).
[23]S. Shi, S. Qian, X. Hou, J. Mu, J. He, and X. Chou, Adv. Condens. Matter Phys. **2018**(1), 7598978 (2018).
[24]G. Angarita, C. Palacio, M. Trujillo, and M. Arroyave, J. Phys.: Conf. Ser. **850**, 012022 (2017).
[25]R. Wang, H. C. Frankis, H. M. Mbonde, D. B. Bonneville, and J. D. B. Bradley, Opt. Mater. **111**, 110692 (2021).
[26]Y. Chiba, Y. Abe, M. Kawamura, and K. Sasaki, Vacuum **83**, 483 (2008).
[27]D. B. Bonneville, H. C. Frankis, R. Wang, and J. D. B. Bradley, Opt. Express **28**, 30130 (2020).
[28]E. S. Magden *et al.*, Opt. Express **25**, 18058 (2017).
[29]J. W. Miller, M. Chesaux, D. Deligiannis, P. Mascher, and J. D. B. Bradley, Thin Solid Films **709**, 138165 (2020).
[30]J. Broßmann, M. Lappschies, S. Jakobs, and V. Kirschner, Proc. SPIE **9627**, 962710 (2015).
[31]S. J. Pearce, M. D. B. Charlton, J. Hiltunen, J. Puustinen, J. Lappalainen, and J. S. Wilkinson, Surf. Coat. Technol. **206**, 4930 (2012).
[32]M. Scherer, J. Pistner, and W. Lehnert, OSA Tech. Dig. **MA7**, 6 (2010).
[33]X. Zhang, J. Zhu, L. Zhang, K. Kishimoto, S. Y. Du, and X. Yin, Surf. Coat. Technol. **228**, S393 (2013).
[34]K. Strijckmans, R. Schelfhout, and D. Depla, J. Appl. Phys. **124**, 241101 (2018).
[35]J. T. Gudmundsson, Plasma Sources Sci. Technol. **29**, 113001 (2020).
[36]S. Berg and T. Nyberg, Thin Solid Films **476**, 215 (2005).
[37]K. Koski, J. Hölsä, and P. Juliet, Surf. Coat. Technol. **116–119**, 716 (1999).
[38]Y. Lan, Y. Zou, X. Ma, L. Xu, L. Shi, and J. Zhang, Mater. Res. Express **7**, 086405 (2020).
[39]Intlvac Thin Film, "Nanochrome IV Thin Film Deposition System"; see https://intlvac.com/Systems/Thin-Film-Deposition/Nanochrome-IV (accessed 4 September 2024).

01 October 2024 14:13:39

Published under an exclusive license by the AVS